Available online at www.sciencedirect.com
ScienceDirect
Procedia Engineering 10 (2011) 965–970
Engineering Procedia

ICM11

Contact fatigue limits of gears, railway wheels and rails determined by means of multiaxial fatigue criteria

E. Conrado[a*], C. Gorla[a]

[a]*Dipartimento di Meccanica, Politecnico di Milano, via G. La Masa 1, I 20156 Milano, Italy*

Abstract

In the present paper, the Dang-Van and the Liu-Zenner multiaxial fatigue criteria are applied to gear and wheel/rail contacts in order to determine contact fatigue limits. In the case of gear contacts, a comparison with experimental contact fatigue limits is discussed for various gear steels. In the case of wheel/rail contacts, the influence of thermal stresses on the contact fatigue limits is analyzed. The results of this analysis are summarized in maps, here called contact fatigue maps, similar to the well-known shakedown maps, but drawn to provide fatigue limits.

Keywords: Rolling contact fatigue; Multiaxial fatigue; Gear contact; Wheel/rail contact; Thermal stresses.

1. Introduction

Rolling contact fatigue (RCF) limits the load-carrying capacity of many important types of mechanical components, such as gears, bearings, rails and railway wheels. Multiaxial fatigue criteria combined with a local approach has been frequently applied to gears, railway wheels and rails for the assessment of contact fatigue limits (see e.g. [1-4]). Recently in [5], a comparison of the results obtained applying the Dang Van, the Crossland and the Papadopoulos criteria to RCF is presented pointing out significant differences between the predicted contact fatigue limits. In [6], maps, called contact fatigue maps and similar to the well-known shakedown maps, but drawn to provide fatigue limits, are introduced in order to make a comparison between shakedown limits and contact fatigue limits obtained by the Dang Van and the Liu-Zenner criteria multiaxial fatigue criteria. In the present paper, the use of these maps for the assessment of contact fatigue limits for gear and wheel/rail contacts is discussed.

* Corresponding author. Tel.: +39-02-2399-8252; fax: +39-02-2399-8202.
E-mail address: edoardo.conrado@polimi.it.

Selection and peer-review under responsibility of ICM11 doi:10.1016/j.proeng.2011.04.159

2. Contact Fatigue limits

In the present paper, the two-dimensional plane strain model of a disc rolling and sliding over a half-plane is used, as a first approximation, to study damage phenomena in gear and wheel/rail contacts. Adopting this model, the stress field induced in the material by the normal and the tangential contact tractions and, thus, the stress time history which undergoes the material of the contacting bodies can be determined by means of analytical formulae (see e.g. [7]). This stress path is a non-proportional one, i.e. the principal stress direction vary with time, implying that the plane of maximum shear stress rotates. Therefore a suitable multiaxial fatigue criterion able to deal with complex multiaxial loading must be applied in order to determine in which conditions fatigue damage initiation occurs. In this paper, the Dang Van and the Liu-Zenner criteria are applied locally at each depth below the contact surface comparing an equivalent stress and an allowable stress for the material in order to determine contact fatigue limits.

2.1. Dang Van and Liu-Zenner Multiaxial Fatigue Criterion

To determine a limit for fatigue crack initiation adopting a multi-scale approach, the Dang Van criterion extends the use of shakedown principles, from the usual macroscopic scale of continuum mechanics to the grain scale, i.e. to the so-called mesoscopic level. It assumes that if an elastic shakedown state is reached at the macroscopic as well as at the mesoscopic scale than the material is not damaged by fatigue. The Dang Van criterion, presented in [8], can be reformulated in a dimensionless form and applied to a line contact problem in order to obtain the ratio $(p_H/\sigma_w)_{E,DV}$ of the maximum Hertzian pressure p_H to the fatigue limit σ_w in fully reversed tension/compression at onset of fatigue damage:

$$\left(\sigma_w / p_H\right)_{E,DV} = \min_{\bar{y}\in\mathbb{R}_0^+} \max_{\bar{x}\in\mathbb{R}} \left\{ a_{DV}\bar{\tau}_{DV}\left(\bar{x},\bar{y}\right) + b_{DV}\bar{\sigma}_H\left(\bar{x},\bar{y}\right) \right\} \tag{1}$$

where a_{DV} and b_{DV} are two material parameters that depend only on the ratio of torsional to axial fatigue limits under fully reversed loading (τ_w/σ_w) being

$$a_{DV} = \left(\tau_w/\sigma_w\right)^{-1} \quad \text{and} \quad b_{DV} = 3\left[1-\left(1/2\right)\left(\tau_w/\sigma_w\right)^{-1}\right] \tag{2}$$

$\bar{\sigma}_H\left(\bar{x},\bar{y}\right)$ is the instantaneous hydrostatic stress and $\bar{\tau}_{DV}\left(\bar{x},\bar{y}\right)$ is the instantaneous maximum shear stress normalized by p_H and calculated from the alternated part of the deviatoric stress tensor:

$$\bar{\sigma}_H\left(\bar{x},\bar{y}\right) = \bar{\sigma}_{kk}\left(\bar{x},\bar{y}\right)/3 \qquad \bar{\tau}_{DV}\left(\bar{x},\bar{y}\right) = \left[\bar{\sigma}'_{a,I}\left(\bar{x},\bar{y}\right) - \bar{\sigma}'_{a,III}\left(\bar{x},\bar{y}\right)\right]/2 \tag{3}$$

being the deviatoric stress tensor and its alternated part respectively defined as:

$$\bar{\sigma}'_{ij}\left(\bar{x},\bar{y}\right) = \bar{\sigma}_{ij}\left(\bar{x},\bar{y}\right) - \left[\bar{\sigma}_{kk}\left(\bar{x},\bar{y}\right)/3\right]\delta_{ij} \quad \text{and} \quad \bar{\sigma}'_{a,ij}\left(\bar{x},\bar{y}\right) = \bar{\sigma}'_{ij}\left(\bar{x},\bar{y}\right) - \bar{\sigma}'_{m,ij}\left(\bar{x},\bar{y}\right) \tag{4}$$

where the mean part of the deviatoric stress tensor $\bar{\sigma}'_{m,ij}$ is calculated according to the minimum circumscribed circle proposal [9] and $\bar{\sigma}_{ij}$ is the state of stress induced by the contact loads normalized by p_H and expressed in a frame of reference moving with the contact loads in which $\bar{x}$ and $\bar{y}$ are, respectively, the surface abscissa and the depth normalized by the semi-width of Hertzian contact b_H.

The Liu-Zenner criterion is an updated version of the so-called *Shear Stress Intensity hypothesis* (SIH) and it is based on the weakest link theory applied to fatigue damage of metals. The Liu-Zenner criterion, presented by Liu in [10], can be expressed in a dimensionless form and applied to contact problems in order to obtain contact fatigue limits as follows:

$$\left(\sigma_w / p_H\right)_{E,SIH} = \min_{\bar{y}\in\mathbb{R}_0^+} \left\{ n_{SIH}\bar{\sigma}_{vm}\left(\bar{y}\right)/2 + \sqrt{n_{SIH}^2\bar{\sigma}_{vm}^2\left(\bar{y}\right)/4 + a_{SIH}\bar{\tau}_{va}^2\left(\bar{y}\right) + b_{SIH}\bar{\sigma}_{va}^2\left(\bar{y}\right) + m_{SIH}\bar{\tau}_{vm}^2\left(\bar{y}\right)} \right\} \tag{5}$$

where σ_{va} and τ_{va} are respectively defined as the quadratic average values of normal and tangential stress amplitude over a unit sphere; τ_{vm} is the quadratic average of the mean tangential stress over a unit sphere weighted by the square of the tangential stress amplitude, while σ_{vm} is the linear average of the mean normal stress weighted by the normal stress amplitude in order to take into account the difference between tensile and compressive normal stresses. All these quantities are normalized by the Hertzian pressure p_H. The dimensionless material parameters a_{SIH}, b_{SIH}, m_{SIH} and n_{SIH} depend only on the ratio of torsional to axial fatigue limits under fully reversed loading (τ_w/σ_w) and pulsating loading (τ_{w0}/σ_{w0}):

$$a_{SIH} = (1/5)\left[3(\tau_w/\sigma_w)^{-2} - 4\right] \qquad m_{SIH} = (7/4)(\tau_w/\sigma_w)^{-2}\left[(1/4)(\sigma_w/\sigma_{w0}+1)^2 - 1\right]$$
$$b_{SIH} = (1/5)\left[6 - 2(\tau_w/\sigma_w)^{-2}\right] \qquad n_{SIH} = (7/5)\left[(\sigma_w/\sigma_{w0}) - (\sigma_{w0}/\sigma_w)(1+4m_{SIH}/21)\right] \tag{6}$$

where the relation between the fatigue limits τ_w and τ_{w0} proposed in [11] is assumed.

2.2. Contact fatigue maps

The dimensionless material parameters of the Dang Van and the Liu-Zenner criteria depend only on the ratio (τ_w/σ_w) and on the mean stress sensitivity $M_\sigma:=(\sigma_w/\sigma_{w0}-1)$. The dimensionless stress field depends only on the coefficient of friction μ, assuming the Poisson's ratio ν equal to 0.3 for steel. Therefore, for a given material, the dimensionless contact fatigue limits can be obtained according to Eq.(1) and Eq.(5) and can be plotted against the coefficient of friction μ to obtain maps, similar to the well-known shakedown maps, but drawn to provide contact fatigue limits.

These maps are shown in Fig.1(a) for the Dang Van and the Liu-Zenner criteria and, for each criterion, considering two values of the ratio (τ_w/σ_w), ($1/\sqrt{3}$) and ($\sqrt{3}/2$), that are, respectively, the lower and the upper limits of the range of applicability of the Liu-Zenner criterion. These fatigue limits for the Liu-Zenner criterion are calculated for values of the mean stress sensitivity equal to $M_\sigma:=1-(1/2)(\tau_w/\sigma_w)^{-1}$ that are the values implicitly assumed by the Dang Van criterion.

For materials with a ratio $(\tau_w/\sigma_w)=(1/\sqrt{3})$ the two criteria give similar results for high values of the coefficient of friction, when the fatigue damage is governed by surface stresses. On the contrary, for low values of the coefficient of friction, when the fatigue damage initiation is expected to be located below the contact surface, the limits given by the two criteria differ significantly: in particular, the Liu–Zenner criterion is more conservative than the Dang Van criterion. Moreover the two criteria predict different values of the coefficient of friction, $\mu_{DV}=0.13$ and $\mu_{SIH}=0.24$, at which the transition from sub-surface and surface damage initiation occurs.

For materials with a ratio $(\tau_w/\sigma_w)=(\sqrt{3}/2)$, the results for the two criteria are completely different. The Dang Van fatigue limits are increased till a maximum of *8* for frictionless contacts. The Liu–Zenner limits, instead, decrease and the maximum value is equal to *1.3* in the case of frictionless contact. Nevertheless both criteria predict that damage initiation occurs always at the surface.

3. Gear contacts

During gear meshing, the tooth flanks are subjected to a moving distribution of contact tractions that can be determined modeling spur gear meshing as a sequence of quasi-static rolling/sliding contacts between equivalent cylinders. These contact loads result in the generation of cyclic contact stresses in the material of gear teeth that are responsible of contact fatigue damage (pitting) and that can be determined by the model of an elastic half-plane subjected to a moving distribution of contact tractions previously described. Thus, contact fatigue limits for spur gears can be obtained from the contact fatigue maps presented knowing the coefficient of friction between gear teeth and the fatigue limit of the gear material.

In Fig.1(b), the results obtained by means of contact fatigue maps for through hardened carbon and alloy steels are compared with the allowable contact number given by the standard ISO 6336-5 [12] that are the synthesis of experimental data obtained from tests performed on gears. In order to make this comparison the coefficient of friction was assumed equal to 0.04, typical for oil lubricated gears, and the fatigue limits of gear steels are derived from hardness values. In particular the conversion from hardness to ultimate tensile strength is performed according to the standard ISO [13] and a ratio of the ultimate strength to the fatigue limit equal to 0.45 as proposed in [14] for steels is assumed. As can be seen from Fig.1(b), the Dang Van criterion with a ratio $(\tau_w/\sigma_w)=(1/\sqrt{3})$ overestimates the contact fatigue limits for the gear steels considered. On the contrary, the fatigue limits obtained by means of the Liu-Zenner criterion varying the ratio (τ_w/σ_w) span nearly the same range given by the ISO for materials with different quality grades.

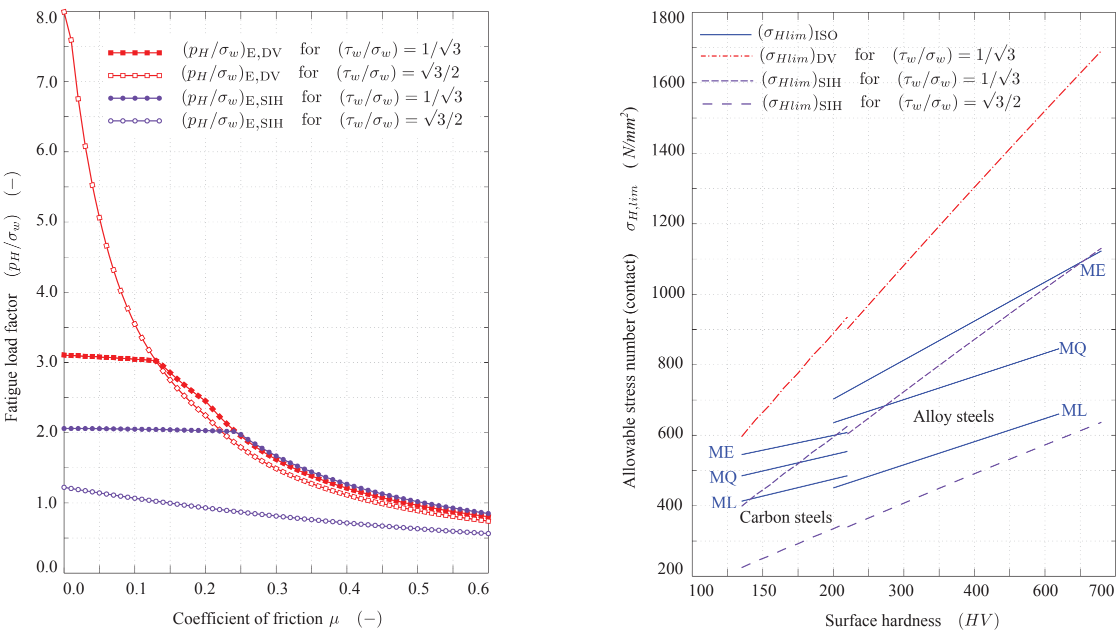

Fig. 1. (a) Fatigue maps for isothermal line contacts; (b) Comparison of contact fatigue limits for gears given in the standard ISO 6336 and obtained by means of multiaxial fatigue criteria for through hardened steels.

4. Wheel-rail contacts

The contact fatigue maps shown in Fig.1(a) can be used also to determined contact fatigue limits of railway wheels and rails. Nevertheless, in this case, the thermal stresses generated at the contact interface between the wheel and the rail due sliding friction should be taken into account since they can be particularly severe at typical wheel/rail contact operating conditions as pointed out in [15]. In fact in wheel/rail contacts heat is generated by sliding friction and flows through the contact surfaces in the material of the contacting bodies causing an increase of the temperature confined in a very thin surface layer. Moreover the bulk temperature of the wheel increases over time due to the periodical frictional heating at its surface. Therefore the bulk temperature of the wheel and the rail are different causing a heat conduction from the wheel into the rail along the contact patch and leading to different surface temperature variations for the wheel and the rail (see [15]). The increase of the surface temperature results in the generation of severe thermal stresses at the surface of the contacting bodies. A compressive equibiaxial stress state acts at the surface that is proportional to the surface temperature and that can be calculated by means of analytical formulae given in [15]. This thermal stress state depends, besides the coefficient of friction μ, only on two others dimensionless parameters. The first one is the dimensionless parameter J defined in [15], that depends on the operating conditions of wheel/rail contacts and that for this kind of contacts is usually in the range 5-10. The other one is the ratio of the actual bulk temperature of the wheel to the bulk temperature of the wheel in a steady-state condition that is reached only after a very long operating time. Different contact fatigue maps can be drawn for various values of these dimensionless parameters, superimposing the thermal stresses to the mechanical stresses induced by the contact loads and using the formulae given in previous section.

In Fig. 2(a), the contact fatigue limits according to the Dang Van and the Liu-Zenner criteria for a material with a ratio $(\tau_w/\sigma_w)=(1/\sqrt{3})$ considering the dimensionless parameter J=5 and equal bulk temperatures for the wheel and the rail are shown. In addition to the isothermal limit curve, two curves are shown: one corresponding to a negative sliding condition, i.e. in the condition when tangential tractions are opposite to the rolling direction, and the other one for a positive sliding condition. Negative and positive sliding conditions correspond for the wheel to braking and driving conditions, respectively, and the opposite for the rail. These two conditions lead to different contact fatigue limits. In the case of negative sliding, the value of the coefficient of friction corresponding to the transition between sub-surface and surface initiation of fatigue damage is reduced. For friction coefficients below this value, fatigue limits are not influenced by thermal effects since the thermal induced stress field is confined at the surface. On the contrary, for higher friction coefficients, the fatigue limits are significatively reduced in comparison with the isothermal case due to the thermal stresses at the surface. In the case of positive sliding, the transition between sub-surface and surface fatigue initiation is shifted to higher values of the coefficient of friction than in the case of isothermal contacts. Contact fatigue limits are slightly increased when fatigue occurs at the surface.

In Fig.2(b) the results, obtained taking into account a bulk temperature of the wheel different from the one of the rail and corresponding to a steady-state condition, are shown. It can be clearly seen that the lowest contact fatigue limits are obtained for the rail during driving, i.e. in a negative sliding condition.

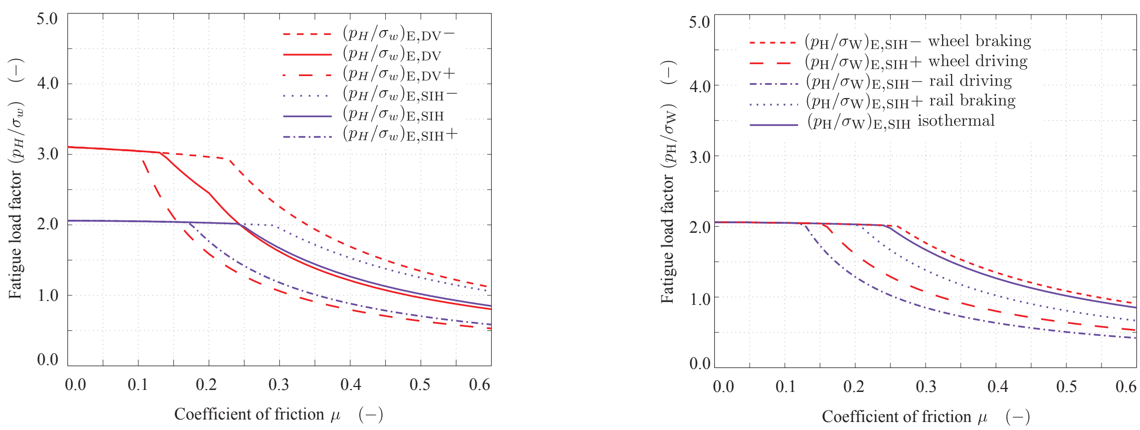

Fig. 2. Fatigue maps for thermo-elastic line contacts for a material with a ratio $(\tau_w/\sigma_w)=(1/\sqrt{3})$ and J=5 (a) Dang Van and Liu-Zenner criteria for equal bulk temperature of wheel and rail; (b) Liu-Zenner criterion for increased steady state bulk temperature of the wheel. ± positive and negative sliding condition.

Moreover these contact fatigue limits are lower than in the case when an initial temperature of the wheel is not taken into account and also the value of the coefficient of friction at which the transition between surface and sub-surface fatigue initiation occurs is further reduced.

5. Conclusions

In this paper, the Dang Van and the Liu-Zenner multiaxial fatigue criteria are used to determine fatigue limits for gear and wheel/rail contacts.

In the case of gear contacts, it is shown that contact fatigue limits in reasonable agreement with the values provided by the standard ISO 6336 for through hardened carbon and alloy gear steels can be obtained by means of the use of the Liu-Zenner multiaxial fatigue criterion. On the contrary, the widely used Dang Van criterion overestimates the contact fatigue limits for these materials.

In the case of wheel/rail contacts, it is shown that thermal stresses, generated by sliding friction, can have a significant influence on contact fatigue limits of both railway wheels and rails. In particular, it is shown that negative and positive sliding conditions result in different contact fatigue limits and that an increased bulk temperature of the wheel can lead to reduced contact fatigue limits for the rail.

References

[1] Ekberg A, Kabo E, Andersson H. An engineering model for prediction of rolling contact fatigue of railway wheels. *Fatigue Frac Engng Mater Struct* 2002;**25**:899–909.

[2] Bernasconi A, Filippini M, Foletti S, Vaudo D. Multiaxial fatigue of a railway wheel steel under non-proportional loading. *Int J Fatigue* 2006;**28**:663–672.

[3] Batista A C, Dias A M, Lebrun J L, Le Flour J C, Inglebert G. Contact fatigue of automotive gears: evolution and effects of residual stresses introduced by surface treatments. *Fatigue Frac Eng Mater Struct* 2000;**23**:217–228.

[4] Tobie T, Hohn B-R, Oster P. Case depth and load capacity of case carburized gears. In Proceeding of the Fourth World Congress on Gearing and Power Transmission, Paris, 1999 p.663–672.

[5] Ciavarella M, Monno F. A comparison of multiaxial fatigue criteria as applied to rolling contact fatigue. *Tribol Int* 2010;**43**:2139–2144.

[6] Conrado E, Foletti S, Gorla C, Papadopoulos I V. Use of multiaxial fatigue criteria and shakedown theorems in thermo-elastic rolling-sliding contact problems. *Wear* 2011;**270**:344–354

[7] Johnson K L. *Contact mechanics*. 1st ed. cambridge: Cambridge University Press; 1985.

[8] Dang Van K, Macro-micro approach in high-cycle multiaxial fatigue. In: McDowel D. L., Ellis R.,editors. *Advances in multiaxial fatigue, ASTM STP 1191,* Philadelphia: American Society for Testing and Materials; 1993, p. 120–130.

[9] Papadopoulos I V. Critical plane approach in high-cycle fatigue: on the definition of the amplitude and mean value of the shear stress acting on the critical plane. *Fatigue Fract Eng Mater Struct* 1998;**21**:269–285.

[10] Liu J. Weakest link theory and multiaxial criteria. In: *Proceeding of the 5th International Conference on Biaxial/Multiaxial Fatigue and Fracture*, Cracow, 1997, p. 45–62.

[11] Zenner H, Simbürger A, Liu J. On the fatigue limit of ductile metals under complex multiaxial loading. *Int J Fatigue* 2000;**22**:137–145.

[12] ISO 6336-5:2003(E). *Calculation of load capacity of spur and helical gears – Part 5: Strength and quality of materials.*. 2nd ed. ISO International Standard; 2003.

[13] ISO 18265:2003(E). *Metallic materials – conversion of hardness values*. 1st ed. ISO International Standard; 2003.

[14] FKM Guideline. *Analytical strength assessment of components in mechanical engineering*. 5th ed. Frankfurt: VDMA Verlag; 2003.

[15] Ertz M, Knothe K. Thermal stresses and shakedown in wheel/rail contact. *Arch Appl Mech* 2003;**72**:715–729.